

Article

Flexible Miniaturized Electrochemical Sensors Based on Multiwalled Carbon Nanotube-Chitosan Nanomaterial for Determination of Nitrite in Soil Solutions

Ana-Maria Gurban ^{1,*}, Lucian-Gabriel Zamfir ¹, Petru Epure ², Ioana-Raluca Șuică-Bunghez ¹, Raluca Mădălina Senin ¹, Maria-Luiza Jecu ¹, Maria Lorena Jinga ¹ and Mihaela Doni ^{1,*}

¹ National Research & Development Institute for Chemistry & Petrochemistry—ICECHIM, 202 Spl. Independentei, 060021 Bucharest, Romania; lucian.zamfir@icechim.ro (L.-G.Z.)

² EPI-SISTEM SRL, 17A Livezii, Săcele, 505600 Brașov, Romania

* Correspondence: ana-maria.gurban@icechim.ro (A.-M.G.); mihaela.doni@icechim.ro (M.D.); Tel.: +40-213-163-063 (M.D.)

Abstract: Flexible screen-printed electrodes (SPE) were modified in a simple manner with different composite nanomaterials based on carbon allotropes, polymers, and metallic nanoparticles, for amperometric detection of nitrites in soil. Multiwalled carbon nanotubes (MWCNT), chitosan (CS), silver nanoparticles (AgNPs), 1,8-diaminonaphthalene (1,8-DAN), and a sol-gel (SG) matrix were used for modification of the carbon paste working electrodes. Sensitive and selective detection of nitrite was achieved by using a MWCNT-CS-modified sensor, in acetate buffer at pH 5, at an applied potential of 0.58 V vs. Ag/AgCl. The MWCNT-CS-based sensor displayed a specific sensitivity of 204.4 mA·M⁻¹·cm⁻², with a detection limit of 2.3 μM (S/N = 3) in a linear range up to 1.7 mM, showing good stability, reproducibility, and selectivity towards other interfering species. A miniaturized portable system using the developed flexible electrochemical MWCNT-CS-based sensors was dedicated for the detection of nitrite in different samples of soil solutions extracted by using suction lysimeters.

Keywords: flexible sensors; MWCNT-chitosan nanocomposite; nitrite; soil solution; lysimeter



Citation: Gurban, A.-M.; Zamfir, L.-G.; Epure, P.; Șuică-Bunghez, I.-R.; Senin, R.M.; Jecu, M.-L.; Jinga, M.L.; Doni, M. Flexible Miniaturized Electrochemical Sensors Based on Multiwalled Carbon Nanotube-Chitosan Nanomaterial for Determination of Nitrite in Soil Solutions. *Chemosensors* **2023**, *11*, 224. <https://doi.org/10.3390/chemosensors11040224>

Academic Editor: Alexander G. Bannov

Received: 26 February 2023

Revised: 27 March 2023

Accepted: 3 April 2023

Published: 5 April 2023



Copyright: © 2023 by the authors. Licensee MDPI, Basel, Switzerland. This article is an open access article distributed under the terms and conditions of the Creative Commons Attribution (CC BY) license (<https://creativecommons.org/licenses/by/4.0/>).

1. Introduction

Nitrite represents an essential plant nutrient and an important part of the plant nitrogen cycle. Nitrite is the most important marker of the nitrification process, and its accumulation in soils can lead to eutrophication bodies of water and growth of toxic algae, being harmful to animals and humans in high concentrations [1]. The nitrification process consists in biological oxidation of the ammonium (NH₄⁺) to highly mobile nitrate (NO₃), via nitrite (NO₂⁻), with this process being carried out mainly by the ammonium-oxidizing bacteria (*Nitrosomonas* sp. and *Nitrobacter* sp.) present in the soil microbial population. In agriculture systems based on the use in excess of chemical fertilizers, rapid and uncontrolled nitrification results in an inefficient nitrogen (N) use by crops, in this way increasing the nitrogen leakage and environmental pollution. Thus, the detection of nitrite, as an indicator of the nitrification process, is of great importance for environmental and agricultural applications [2].

There are numerous analytical methods proposed for nitrite quantification which encompass sophisticated and centralized techniques, such as spectrophotometry [3], high-performance liquid chromatography [4], ion chromatography [5], fluorescence spectroscopy [6], chemiluminescence [7], and capillary electrophoresis [8]. These methods have shown important limitations, such as sample pretreatment, susceptibility to matrix interferences, insufficient detection limits, time-consuming, often requiring expensive bulky equipment, large volumes of reagents and samples, needing to be operated by specialized personnel, lack of portability, and a lack of ability for in situ nitrite determination.

The electrochemical methods are advantageous over the other methods in terms of cost and time. Electrochemical sensors offer a promising alternative to traditional detection methods due to their potential for miniaturization, portability, and on-site determination of a variety of analytes [9]. Especially, ion-selective electrodes were commercialized, and among them the ones for nitrate and nitrates, but they are not sufficiently robust and cannot achieve low limits of detection [10].

Electrochemical determination of nitrite is performed, either by reduction or oxidation, but the most reported electrochemical methods are the oxidation ones, with the nitrite being directly oxidated at the surface of unmodified working electrodes. Different materials, such as glassy carbon, gold, platinum, or metal oxides, were reported for such type of nitrite sensors [11,12]. The application of these sensors in real conditions is limited, due to the fouling of the sensor surfaces with different species, which resulted in the electrochemical process or was found in the sample matrix. Therefore, research has been focused towards improving the sensitivity and selectivity of nitrite detection, by modification of sensors' surfaces with different materials. Various electrochemical sensors based on iron porphyrin, ruthenium polymer, nitrite reductase, polyaniline/carbon nanotubes composite, and hemoglobin/colloidal gold nanoparticles have been developed for the determination of nitrite, mainly in water (drinking, surface, and waste) and in food [12].

An electrochemical biosensor reported by Quan and Shin [13] for nitrite detection was developed by co-immobilization of copper-based nitrite reductase and redox viologen-chitosan on the glassy carbon electrode. The synthesis of viologen-chitosan compound involved several complex and time-consuming steps, while the co-immobilization process required the use of a polyurethane membrane to ensure the stability of the sensitive layer. Detection of nitrite using the developed biosensor was carried out at -0.75 V, at pH 6.5 under argon flow, with a sensitivity of $0.21 \mu\text{A} \cdot \mu\text{M}^{-1} \cdot \text{cm}^{-2}$. Another biosensor based on a homemade pyrolytic graphite electrode modified with conductive carbon ink and cytochrome c nitrite reductase was reported by Monteiro et al. [14]. The detection of nitrite with such developed biosensor involved a prior electrochemical reduction of the enzyme at a negative potential of -0.8 V and the use of an additional oxygen scavenger system based on glucose oxidase, catalase, and glucose. Despite the sensitivity of $0.55 \text{ A} \cdot \text{M}^{-1} \cdot \text{cm}^{-2}$ displayed by the biosensor and its complexity, there are considerable issues regarding the interaction between the scavenging system and the bioelectrode by creating a passivation layer, which can act as a diffusion barrier to nitrite, thereby decreasing the sensitivity.

The biosensors based on nitrite-reductase present good analytical performances in terms of sensitivities and detection limits, however their complexity and need for standard oxygen removal strategies make them incompatible with in-field measurements. A low detection limit of $0.1 \mu\text{M}$ was obtained for nitrite determination in water by Badea et al. [15] using a flow injection system and a Pt electrode modified with a non-conducting polymer, while another sensitive nitrite sensor based on a carbon paste electrode covered with a cellulose acetate membrane was developed by the same author for nitrite determination in cured meat samples [16]. Both electrochemical sensors were operated at a high overvoltage, being susceptible to interfering compounds.

The overpotential values and the electron-transfer rates obtained for the nitrite oxidation at the surface of unmodified electrode materials lead to a lack of the sensitivity and selectivity required for the electrochemical detection of nitrite. Since the electrode materials play the most important role in the construction of high-performance electrochemical sensing platforms for target molecules' detection, the advance of nanomaterial technology provides great opportunities and possibilities in the design and development of new (bio)sensors. Due to the excellent properties of the nanomaterials, such as shape, size, aggregation/agglomeration state, size distribution, low cost, electroconductivity, the large surface-to-volume ratio and surface-specific area, accelerating the electron transfer, the high possibility for their functionalization, offering flexibility, selectivity, strong stability, and a good biocompatibility, it allows them to provide enhanced interfacial adsorption with improved electrocatalytic activity and faster electron transfer kinetics [17–21]. Some

of the most commonly used nanomaterials are carbon allotropes (e.g., carbon nanotubes, nanofibers, fullerenes, or graphene), metallic nanoparticles, conductive polymers, etc. Carbon-based nanomaterials have been used in the development of sensors due to their high electric conductivity, large active surface area, and ease of functionalization with other materials or active functional groups.

Composite nanomaterials based on carbon nanotubes (single- and multi-walled) and metallic nanoparticles were used to facilitate the transfer of electrons between nitrite anions from the solution and surface of different working electrodes, leading to an augmented signal and improved sensors' sensitivity [22]. Polymeric materials are often used for entrapping nanomaterials on the active surface of the sensors, in this way enhancing the stability and selectivity of the developed sensors. Chitosan (CS) represents a natural polymer with functional amino and hydroxyl groups, that is able to form films on the electrode surface, and which has been widely used in the preparation of composite nanomaterials and in the development of electrochemical sensors [23]. Electrochemical sensors for nitrite determination were developed based on composite materials obtained by functionalization of carbon nanomaterials with metal nanoparticles and chitosan [24–26].

The use of hybrid nanomaterials based on different precursors, such as carbon-based nanomaterials together with metallic nanoparticles [27,28], metallic nanoparticles and polymers [29,30], carbon-based nanomaterials with polymers [31], or all three types of precursors [32], in electrochemical sensors' development, has been reported to enhance the sensitivity towards nitrite.

However, despite an improved sensitivity and a lower limit of detection, the electrochemical detection of nitrite occurred mostly at a relatively high overvoltage, ranging from +0.70 to +0.85 V [33–39], and no application for direct determination of nitrite in soil was developed. The sensor modification often requires extra steps for nanomaterial preparation, such as the synthesis of the carbon-based materials [36] and metal nanoparticles [34,40], or polymer deposition of surfaces [15,16], which can be time-consuming, costly, and may need further optimization studies.

The present work describes a simple, rapid, and efficient amperometric detection of nitrite in soil solution by using flexible and miniaturized electrochemical nanocomposite-based sensors. Screen-printed carbon electrodes were simply modified with different nanocomposite materials, based on MWCNT, silver nanoparticles (AgNP), and different matrices for entrapment of nanomaterials, such as chitosan (CS), 1,8-diaminonaphthalene (1,8-DAN), and sol-gel. Functionalization of MWCNT with AgNP was performed in order to enhance the electrocatalytic behavior of MWCNT toward nitrite oxidation, by decreasing the overpotential and at the same time increasing the sensitivity for nitrite determination at different pH values. The use of different matrices for entrapment of the nanomaterials aimed at the increase of the stability of the nanomaterials at the sensor surface and, respectively, the minimization of interferences from the soil matrix.

Among all the studied materials, flexible sensors developed by using the MWCNT-CS composite showed an increased sensitivity and selectivity for amperometric detection of nitrite in soil solutions extracted with suction lysimeters (soil solution extractors). The developed sensors were used with good accuracy, reproducibility, and selectivity for the determination of nitrite in different local samples of soils.

2. Materials and Methods

2.1. Reagents

Sodium nitrite, sodium nitrate, sodium acetate, acetic acid, low molecular weight chitosan (CS, MW = 50–190 kDa), silver nanoparticles (AgNP, 20 nm particle size, with a dispersion of 0.02 mg/mL in aqueous buffer containing sodium citrate as a stabilizer), 1,8-diaminonaphthalene (1,8-DAN), sodium phosphate dibasic dihydrate ($\text{Na}_2\text{HPO}_4 \cdot 2\text{H}_2\text{O}$), potassium phosphate monobasic (KH_2PO_4), NaCl, KCl, $\text{K}_4\text{Fe}(\text{CN})_6$, $\text{K}_3\text{Fe}(\text{CN})_6$, tetraethyl orthosilicate (TEOS), methyl triethoxysilane (MTEOS), polyethylene glycol 550 monomethyl ether (PEG550), calcium chloride (CaCl_2), urea, glucose, and citric acid were obtained from

Sigma-Aldrich and were of analytical grade. MWCNT was obtained from Future Carbon GmbH, Bayreuth, Germany. The solutions were prepared in ultrapure water (MilliQ, 18.2 M Ω cm). The buffers used for the electrochemical experiments were 0.1 M acetate buffer for pH values 4.0–5.5 and 0.1 M phosphate buffer (PBS) for pH 6.0–7.5. The nitrite and the potential interfering species solutions were freshly prepared with ultrapure water (18.25 M Ω ·cm) just before use.

2.2. Apparatus and Measurements

Electrochemical measurements were carried out with a μ Stat 4000 Multi Potentiostat/Galvanostat and the acquisition of recorded data was carried out with DropView 8400 software. A conventional three-electrode electrochemical cell was used for the experiments, consisting of a system of SPE (DRP-110) on ceramic and PVC supports. The working (4 mm diameter) and counter electrodes were made of carbon, while the reference electrode was represented by a silver pseudo-reference electrode. All the experiments were performed at room temperature. Cyclic voltammetry (CV) experiments have been performed in stationary solutions, by cycling the potential between -0.2 and 1 V, with a scan rate of 0.05 V/s. Amperometric measurements were performed at room temperature, in stirring solutions, with all the potentials being referred to the Ag pseudo-reference electrode. Electrochemical impedance spectroscopy (EIS) measurements were performed with a portable and wireless μ Stat-i 400s (bi)potentiostat/galvanostat in the frequency range of 1 MHz to 10 Hz, with a potential amplitude of 10 mV, at an open circuit potential (OCP) using a solution of 5 mM $\text{Fe}(\text{CN})_6^{4-}/\text{Fe}(\text{CN})_6^{3-}$ prepared in KCl 0.1 M.

Amperometric detection of nitrite in soil solutions was performed with the portable and wireless bi-potentiostat, at different applied potentials depending on the pH of the soil samples. An Elmasonic E30H ultrasonic bath was used for the preparation of the nanocomposite materials.

Morphological studies of modified surfaces of the sensors (based on ceramic support) were carried out with a scanning electron microscope SU-70 (Hitachi, Chiyoda City, Tokyo, Japan) with an energy-dispersive X-ray (EDAS) module, having an accelerating voltage of 4.6 kV, coupled with an Ultra-Dry Thermo Fischer Scientific detector. The data for the particle rugosity were processed using the ImageJ NIH Software. FTIR spectra were recorded using a Bruker Tensor 37 FTIR spectrometer.

Determination of nitrite content in the soil samples before and after the cultivation of the plants was carried out with a UV-VIS CINTRA 202 (GBC Scientific Equipment Pty. Ltd., Dandenong, Australia) spectrophotometer. A HI707 Low-Range Nitrite Colorimeter (Hanna Instruments, Woonsocket, RI, USA) was also used for the validation of the results obtained with the developed sensors.

2.3. Preparation of the Nanocomposite-Modified Sensors

Screen-printed carbon paste electrodes were modified with different nanocomposite materials based on MWCNTs, AgNPs, polymers, and sol-gel matrices. Thus, in a first attempt, MWCNT-CS-based nanocomposite material was obtained by dispersion of 5 mg of MWCNT in 1 mL of chitosan solution, having different concentrations, from 0.1% to 1% , prepared in 2% acetic acid. For preparation of MWCNT-based sensors, MWCNTs were dispersed in 2% acetic acid without CS. The mixtures were sonicated for 1 h at room temperature. Further, volumes of 10 μ L mixtures were drop-casted on the surface of the working electrode. Sensors based on MWCNT-AgNP were prepared by deposition of a 10 μ L suspension of AgNP containing 1 mg/mL of MWCNT onto the active area of the working electrode surface. All these modified sensors were dried at 65 $^\circ\text{C}$ for 1 h and kept at room temperature in a dry place when not in use.

Polymeric-based sensors were obtained by electro-polymerization of the 1,8-DAN monomer onto the already modified MWCNT/SPE, and respectively, MWCNT-AgNP/SPE, according to the methods described by Badea et al. [15]. The electro-polymerization of 1,8-DAN was carried out by cyclic voltammetry, in a potential range of -0.15 to

1.3 V vs. Ag/AgCl, with a scan rate of 0.05 V/s, for 5 cycles, by placing 200 μ L of a 5 mM monomer solution prepared in NaCl 0.2 M, pH 1, onto the surface of the modified sensors.

A sol-gel matrix based on TEOS and MTEOS precursors, in a volumetric ratio of 1:3, was prepared for the modification of MWCNT/SPEs, and respectively, MWCNT-AgNP/SPE-based sensors. After a 6 h hydrolysis time of sol at 4 °C, to allow the formation of the gel, a volume of 5 μ L of sol-gel was drop-casted onto the modified working electrodes. The sol-gel-based modified sensors were kept at 4 °C.

2.4. Real Samples' Measurements

Soil samples were taken at a depth of 50 cm from a corn field, and respectively, from a vegetable garden in the southern region of Romania. The field and garden soil samples were used in the laboratory to cultivate tomato seeds into glass tanks. Low-volume suction lysimeters (Hanna Instruments, 30 cm) for root-level soil monitoring were used to collect the soil solutions that were analyzed. The nitrite concentrations were determined by amperometric measurements using the optimized modified sensors from the soil solution samples, before cultivation and after cultivation of tomatoes.

For spectrophotometric determination of nitrites, the soil samples were dried at room temperature for 24 h, mortared, and passed through a 2 mm sieve. A suspension was obtained by adding ultrapure water in a liquid–solid ratio of 10 L/kg, and after homogenization and decanting solids, the elute was filtered through a 0.45 μ m membrane filter.

2.5. Validation of Measurements from Real Samples

Determination of nitrite content in soil samples was performed according to standardized methods in force SR EN 12457-4:2003, and respectively SR EN 26777-2002 for water quality, using spectrophotometric and colorimetric methods.

The principle of spectrophotometric detection of nitrites is based on the reaction of the nitrite anions from the soil samples with 4-aminobenzenesulfonamide, at a pH of 1.9 in the presence of orthophosphoric acid, in order to form a red-colored complex with N-(1-naphthyl) ethylenediamine dihydrochloride, with the absorbance being measured at 540 nm.

The detection of nitrite using the HI707 Low-Range Nitrite Colorimeter (Hanna Instruments) is based on a colorimetric method, an adaptation of the EPA Diazotization Method 354.1 [41]. The principle of the method consists in following the appearance of the pink color in the soil solution samples at 470 nm, through the diazotization reaction between the nitrites in the samples with certain aromatic amines, in which a diazonium salt is formed that can then be coupled with another amine or phenol to form an intensely colored azo dye.

3. Results and Discussion

3.1. Morphological and Structural Characterizations of Nanomaterials

The surface morphologies of the nanomaterial-based SPE were analyzed using SEM by comparing with that of unmodified SPE (Figure 1).

Figure 1B shows the coverage of the rough surface of the carbon paste working electrode with a thin and relatively homogenous layer of chitosan. Additionally, a uniform distribution of MWCNT onto the SPE surface (Figure 1C) and a more homogenous wrapping of the MWCNTs by the CS layer (Figure 1D) can be observed, providing a more stable and uniform coating of the sensor surface. The roughness of the sensor surface modified with MWCNT-CS increased, which indicates an increase of the electroactive surface area.

In the Supplementary Materials (Figure S1), the morphology of the surface of sensors modified with other nanomaterials based on entrapment of MWCNT can be observed and, respectively, of functionalized MWCNT with AgNPs in poly-1,8-DAN and the SG matrix (Figure S1D,G). In the case of MWCN-AgNP, an agglomeration of the nanoparticles onto the nanotubes was observed (Figure S1A,D), and moreover, a cracking of the layer was evidenced in the case of using the SG matrix for entrapment of the nanomaterial (Figure S1C).

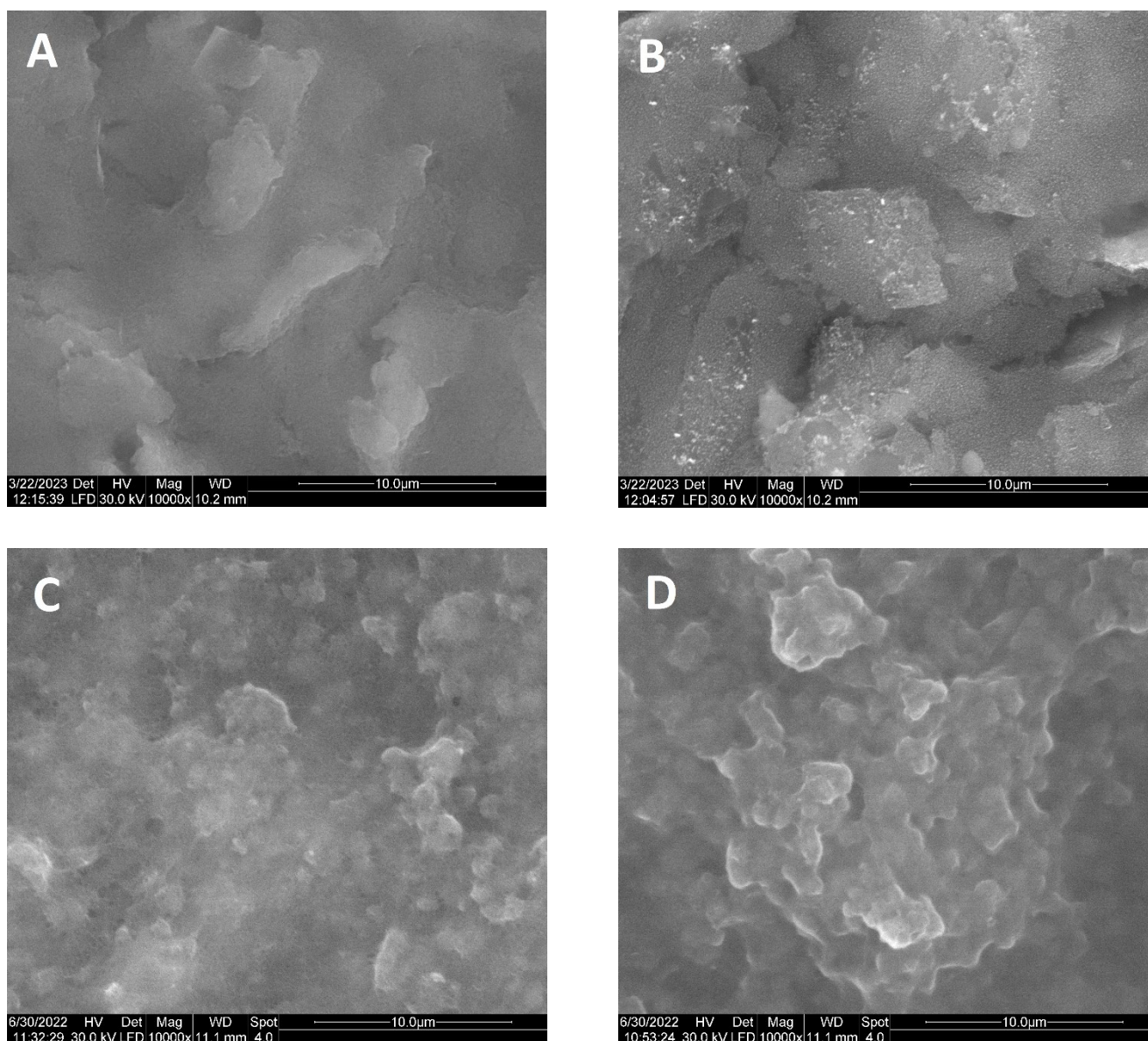


Figure 1. SEM images of: (A) SPE, (B) CS/SPE, (C) MWCNT/SPE, and (D) MWCNT-CS/SPE.

FTIR spectroscopy studies were performed for further characterization of the nanomaterials used for the sensors' modification (Figure 2A,B).

The vibration peak in the MWCNT spectra at 1547 cm^{-1} is attributed to the presence of the C=C bond from the carbon nanotube sidewall, while the band at 1704 cm^{-1} can be attributed to C=O stretching and those at 1225 cm^{-1} to the C–O stretching vibration, indicating the presence of carbonyl and hydroxyl groups on the nanotubes.

The absorption band observed in Figure 2A at 1372 cm^{-1} for CS (d), MWCNT-CS (e), and respectively, MWCNT-AgNP-CS (f), corresponds to the C–N stretching vibration in the amide bonds of chitosan [42]. For the CS spectrum, the absorption peak from 2872 cm^{-1} corresponds to the CH₂ stretching vibration, while the broad band from 3285 cm^{-1} can be attributed to the overlap of N–H and O–H stretching vibrations [43]. The bands recorded at 1573 cm^{-1} and 1638 cm^{-1} can be attributed to the protonated amine vibration and N–H bending vibration in the amide group, respectively.

The band at 1059 cm^{-1} is related to the vibration of CO groups [43]. The vibrational bands that can be seen in Figure 2A for MWCNT are covered by the bands of the CS in

the MWCNT-CS and MWCNT-AgNP-CS mixtures, which confirms that the MWCNT are coated by the CS.

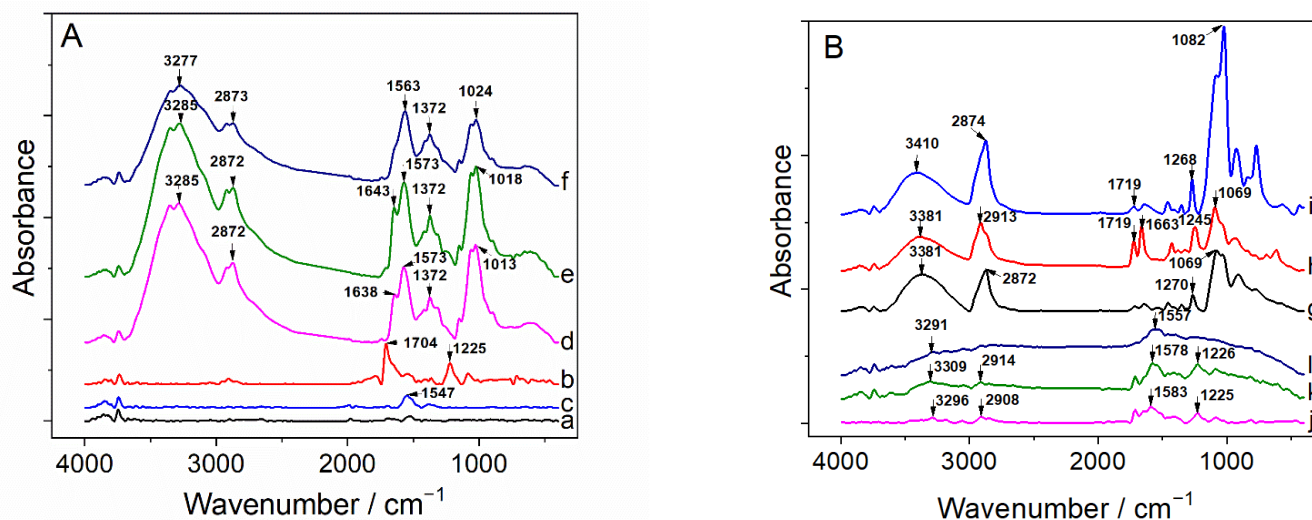


Figure 2. FTIR spectra for: (A) (a) SPE, (b) MWCNT/SPE, (c) MWCNT-AgNP/SPE, (d) CS/SPE, (e) MWCNT-CS/SPE, and (f) MWCNT-AgNP-CS/SPE. (B) (g) SG/SPE, (h) MWCNT-SG/SPE, (i) MWCNT-AgNP-SG/SPE, (j) 1,8-DAN/SPE, (k) MWCNT1,8-DAN/SPE, and (l) MWCNT-AgNP 1,8-DAN/SPE.

The spectra for sensors modified with poly(1,8-DAN) are shown in Figure 2B. The absorption bands at 3296 cm^{-1} , 2908 cm^{-1} , and 1393 cm^{-1} correspond to stretching vibrations of N–H, C–H, and C–N in the secondary amino groups, respectively. The band at 1583 cm^{-1} is related to the C=C stretching vibration in aromatic rings [44].

The presence of the strong band at 1225 cm^{-1} is assigned to the C–C inter-ring stretching vibrations of the bonds between monomer units. The spectra confirm the polymerization of poly(1,8-DAN) and its presence in the composite material layers.

For the SG-modified surfaces, the absorption band at 1270 cm^{-1} can be attributed to the stretching vibrations of C–Si, and the width of the vibration band at 1069 cm^{-1} is related to Si–O–Si stretching vibrations within the SG matrix. The spectrum for MWCNT-AgNP-SG shows the MWCNTs and AgNPs as being embedded by the SG matrix as the bands for MWCNTs are covered by the bands.

3.2. Cyclic Voltammetry Studies

3.2.1. Electrochemical Oxidation of Nitrite at Nanocomposite-Based Sensors

In a first attempt, CV studies were performed using modified sensors based on MWCNT and different matrices, using PBS 0.1 M, pH 7, in the presence of 1 mM of nitrite, by cycling the potential between -0.2 and 1 V vs. Ag/AgCl, with a scan rate of 0.05 V/s . The peak potential and current intensity for the oxidation of 1 mM of nitrite were recorded for SPE sensors modified with MWCNT (1 mg/mL), CS (0.5%), poly(1,8-DAN), and SG matrices (Figure 3).

It can be clearly noticed that through modification of SPE surfaces with MWCNT-CS nanomaterial, the oxidation of nitrite occurred in neutral medium, at the potential of 0.748 V , producing an anodic peak current of $27.3\text{ }\mu\text{A}$ (curve b). For the sensors modified only with MWCNT, the oxidation of nitrite occurred at a higher value of potential, 0.813 V , with the intensity current of the anodic peak being $21.45\text{ }\mu\text{A}$ (curve a). By entrapping the MWCNT in the electropolymerized film of 1,8-DAN, no electrocatalytic activity was recorded (curve c).

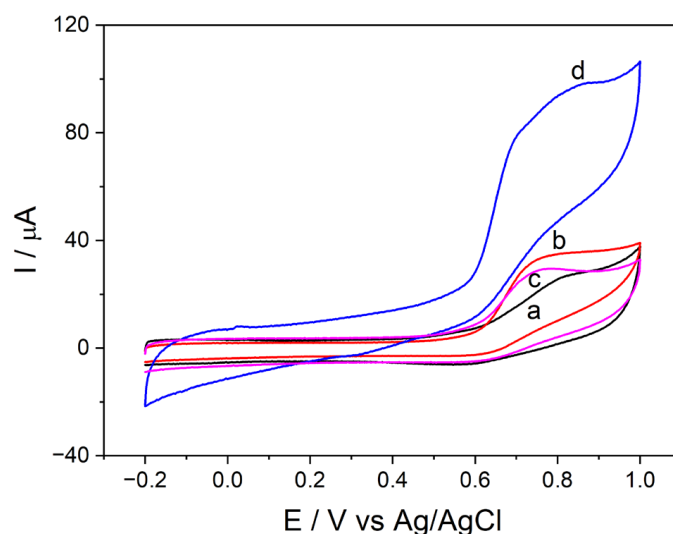


Figure 3. Cyclic voltammograms recorded for: MWCNT/SPE (a), MWCNT-CS/SPE (b), MWCNT-1,8-DAN/SPE (c), and MWCNT-SG/SPE (d) (PBS 0.1 M, pH 7, $v = 0.05$ V/s).

In the case of the sensors modified by entrapment of MWCNT in the SG matrix, although an improvement of the electrocatalytic activity was expected (curve d), this was not sustained by the further studies carried out.

Cyclic voltammograms of SPE modified by entrapment of functionalized MWCNT-AgNP in different matrices, recorded in the same conditions as described above, are presented in Supplementary Material (Figure S2). By functionalization of MWCNT with AgNPs, the electrocatalytic activity of sensors considerably increased (Figure S2-curve a), with the oxidation of nitrite occurring at 0.856 V, with an intensity of the anodic peak current of 76.1 μA .

By using the 1,8-DAN electropolymerized film to entrap MWCNT-AgNP (Figure S2-curve c), no obvious modifications of the electrocatalytic activity were observed, compared with MWCNT-1,8-DAN/SPE (Figure 3, curve c). For the sensors modified with MWCNT-AgNPs and the SG matrix, a slight improvement of the electrocatalytic behavior was observed. The sensors developed by entrapment of nanomaterials into the SG matrix showed poor stability, with several cracks also being evidenced by SEM images. For this reason, MWCNT-SG/SPE and, respectively, MWCNT-AgNP-SG/SPE were not used for further studies.

The MWCNT-CS-modified sensors showed an enhanced electrocatalytic behavior towards nitrite oxidation, in terms of lowering the oxidation potential value, with an increase of the intensity of the anodic peak current. The stability of the nanomaterial at the sensor surface was considerably improved via the use of chitosan. Thus, MWCNT-CS was used in the further electrochemical studies toward the oxidation of nitrite.

Electrocatalytic oxidation of nitrite at the surface of unmodified and modified sensors with 5 mg/mL of MWCNT and CS 0.5% was studied in acetate buffer 0.1 M, pH 5, containing different concentrations of nitrite (Figure 4A,B).

The voltammograms showed a decrease of the oxidation potential value from 0.725 V for bare SPEs to 0.51 V for MWCNT-CS/SPE. The peak current intensity for the oxidation of nitrite on MWCNT-CS/SPE was 113 μA , compared to 70.5 μA recorded with the sensors based only on MWCNT, proving a higher sensitivity for the composite nanomaterial based on MWCNT and chitosan 0.5%. The increase of the MWCNT-CS/SPE sensors' sensitivity is explained by the conversion of the $-\text{NH}_2$ group in the chitosan matrix into $-\text{NH}_3^+$ at acidic pH values, which facilitates the absorption of nitrate anions on the sensor surface. Additionally, the high current intensity and low potential values for the MWCNT-CS/SPE sensors demonstrate the synergistic effects of MWCNTs and CS.

An increase of the oxidation current with the increase of the nitrite concentration can be observed in Figure 4B, from 46 μA recorded in the presence of 0.5 mM of nitrite

to a value of 368 μA for 5 mM of the substrate, with a concomitant shift of the oxidation potential towards more positive values, from 0.51 V to 0.62 V.

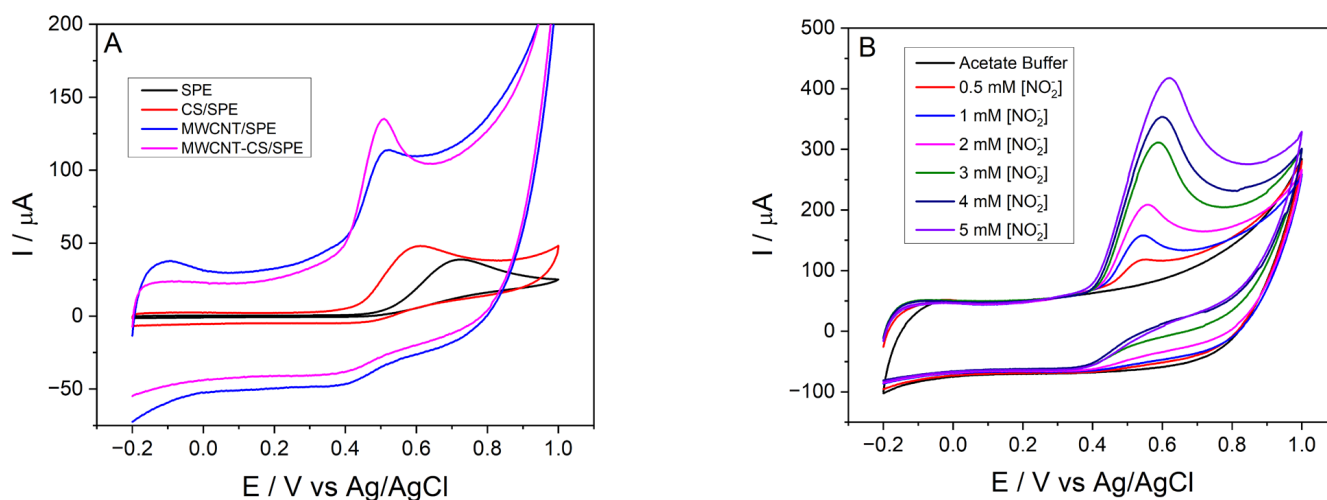


Figure 4. Cyclic voltammograms recorded for oxidation of: (A) 1 mM of nitrite on bare SPE- (a), CS/SPE- (b), MWCNT/SPE- (c), and MWCNT-CS/SPE-based sensors (d), and (B) 0.5, 1, 2, 3, 4, and 5 mM of nitrite on MWCNT-CS/SPE (acetate buffer 0.1 M, pH 5, $\nu = 0.05$ V/s).

In order to avoid the sensor surface poisoning, the regeneration of the MWCNT-CS-based sensor after multiple uses was performed in CV, by cycling the potential in a reverse way, from +1 to -1.2 V vs. Ag/AgCl, with a scan rate of 0.05 V/s for 12 cycles (Figure 5).

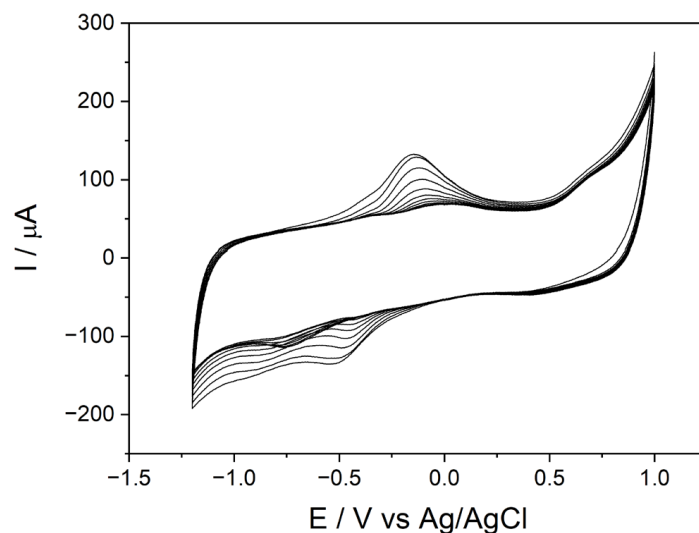


Figure 5. Regeneration of MWCNT-CS-based sensors (acetate buffer 0.1 M, pH 5, $\nu = 0.05$ V/s, $n = 12$ cycles).

Electrodes are usually subjected to changes at their surface when used in electrochemical oxidation and reduction reactions. In addition, contaminants in the samples are oxidized at the surface of the electrodes, rendering the electrodes ineffective, so that after a period of time, the sensors no longer properly function.

It was observed that the anodic and cathodic peaks corresponding to the oxidation of adsorbed nitrate that was formed on the surface of the electrode decreased in intensity until their disappearance, thus demonstrating the regeneration of the sensor surface modified with the nanomaterial composite.

3.2.2. Effect of Scan Rate on the MWCNT-CS/SPE

Selection of the working applied potential is of great importance in order to achieve a good sensitivity and a low detection limit, while minimizing the interferences. For that purpose, the behavior of MWCNT-CS/SPE and the variation of the oxidation potential were studied in the same conditions as described before, by cycling the potential with different scan rates, from 0.025 to 0.3 V/s (Figure 6A–C).

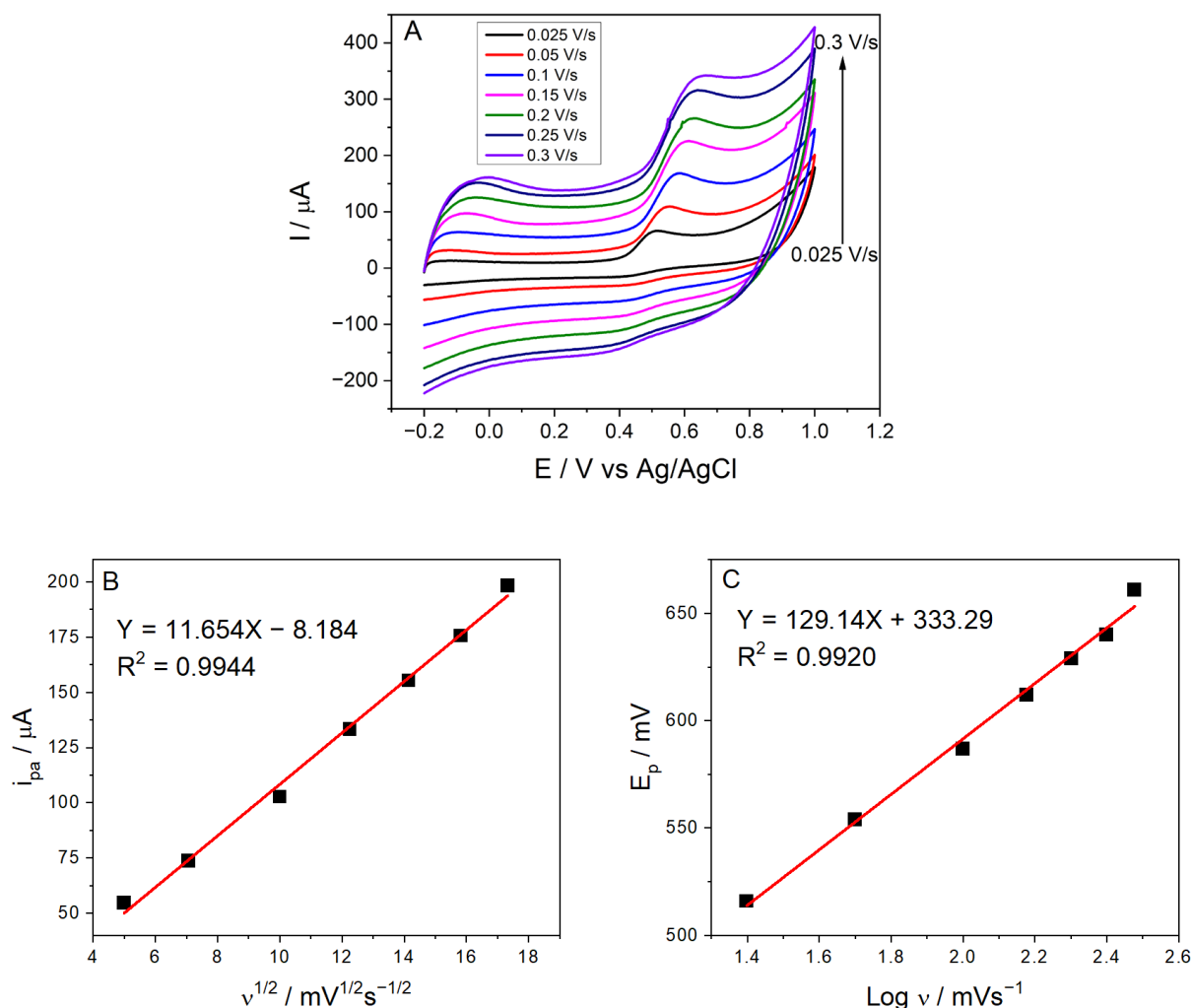


Figure 6. (A) Cyclic voltammograms performed with MWCNT-CS/SPE at different scan rates (acetate buffer 0.1 M, pH 5, 1 mM nitrite, scan rate 0.025; 0.05; 0.1; 0.15; 0.2; 0.25 and 0.3 V/s). (B) Plot of anodic peak current (I_{pa}) vs. square root of the scan rate ($v^{1/2}$). (C) Plot of anodic potential (E_p) vs. log of the scan rate ($\log v$).

A proportional variation of the oxidation potential with the scan rate, as well as an increase of the anodic peak currents with the increase of the scan rate, were also observed. The oxidation potential shifted towards more positive values, indicating the existence of a kinetic limitation between the MWCNT-CS/SPE and nitrite.

3.2.3. Effect of pH

The electrochemical behavior of the MWCNT-CS layer towards oxidation of nitrite was evaluated by CVs using different buffer solutions, with pH ranging from 4 to 9, in the presence of 1 mM of nitrite with a sweep rate of 0.05 V/s (Figure 7A).

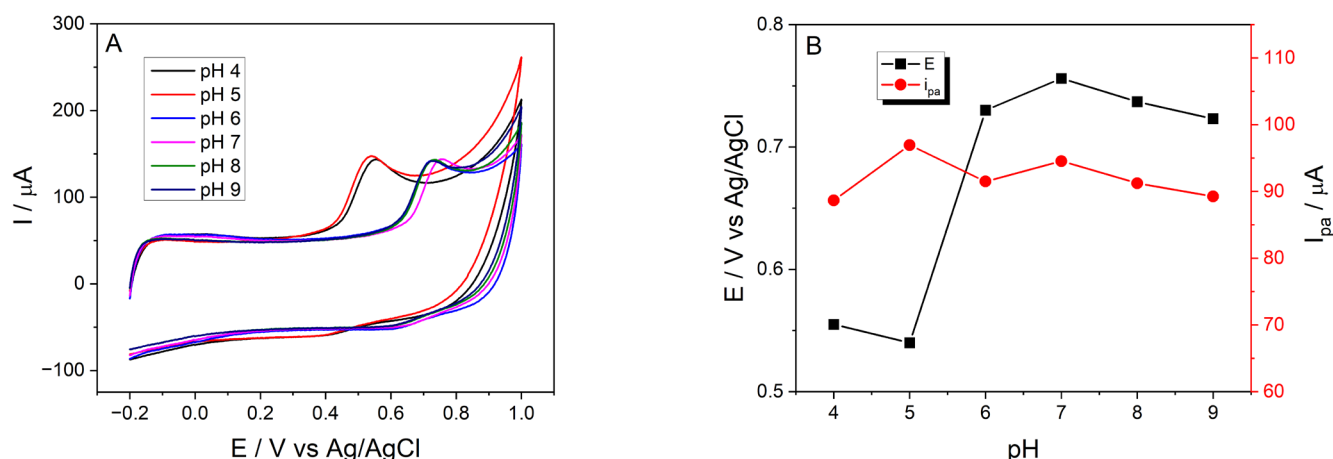


Figure 7. The effect of pH on the electrocatalytic behavior of MWCNT-CS/SPE: (A) cyclic voltammograms in acetate and PBS buffers containing 1 mM of nitrite, and (B) variation of oxidation peak potential and current vs. pH.

The MWCNT-CS nanomaterial has been shown to be highly electroactive towards nitrite oxidation, especially at pH 5, while at neutral and alkaline pH, the activity decreased. As shown in Figure 7B, the anodic peak current of MWCNT-CS for nitrite oxidation increased by increasing the pH up to 5, and then slightly decreased as the pH increased. This behavior can be explained by the fact that the pK_a of HNO₂ is 3.3, and most nitrite anions are protonated in acidic solutions [45,46]. In alkaline medium, the formation of oxides at the electrode surface is favored, leading to an inhibition of the oxidation of nitrites [47]. The amino groups from CS can convert into positively charged -NH₃⁺ at low pH values, in this way facilitating the interaction with nitrite anions. The potential of the oxidation peak shifts to more positive values with the increase of the pH value.

It can be concluded that the electron transfer at the surface of modified sensors with nanomaterial based on MWCNT and chitosan was favored in acidic medium. Taking into consideration the results obtained in the CV studies, a pH value of 5 was considered optimal for the subsequent amperometric measurements.

3.2.4. Effect of MWCNT Loading in the Composite Material

The composition of the nanocomposite material was optimized in order to achieve a high sensitivity and selectivity for nitrite detection (Figure 8A,B).

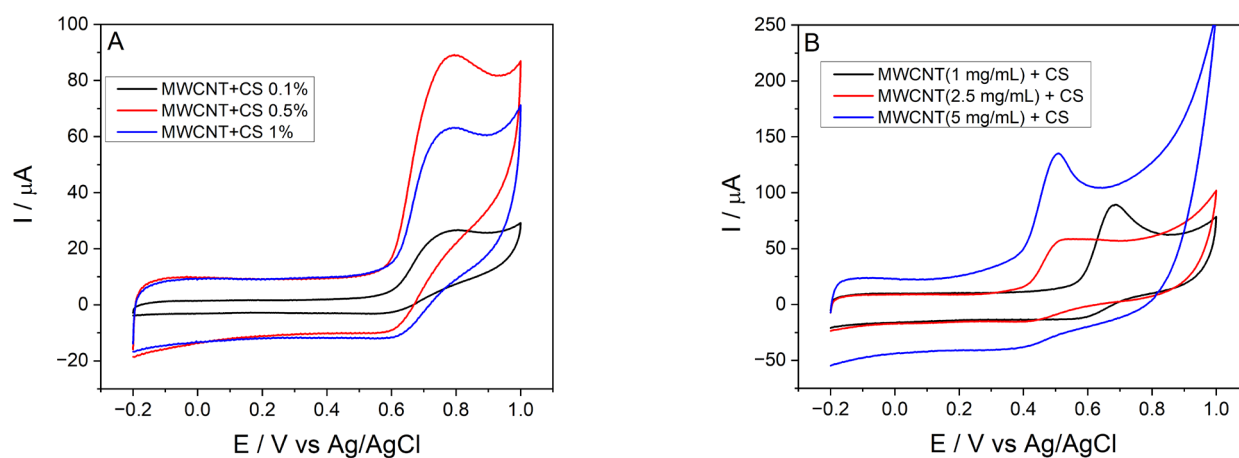


Figure 8. Cyclic voltammograms recorded with MWCNT-CS-based sensors: (A) MWCNT 1 mg/mL and CS (0.1; 0.5 and 1%), and (B) MWCNT (1; 2.5 and 5 mg/mL) and CS 0.5% (acetate buffer 0.1 M, pH 5.0, 1 mM nitrite, scan rate of 0.05 V/s).

The concentration of CS used in the composite mixture was optimized by comparing the responses of the sensor toward 1 mM of nitrite, with the highest current intensity being observed when 0.5% CS was used (Figure 8A). A higher concentration of 1% CS could hinder electron and ion transfer on the surface of the sensor due to the increase of the layer thickness on the working electrode, while 0.1% CS provided less positively charged amino groups on the surface compared to 0.5% CS. For these reasons, a concentration of 0.5% CS was considered optimal.

The MWCNT loading on the modified sensors influenced the electrochemical response by lowering the oxidation potential from 0.686 V obtained for the use of 1 mg/mL of MWCNT to 0.51 V when 5 mg/mL of MWCNT was used (Figure 8B). A higher amount of MWCNT, as much as 7 or 10 mg/mL, led to an increase of the background noise. Thus, 5 mg/mL of MWCNT was chosen as the optimum for sensors' modification.

3.3. Electrochemical Impedance Spectroscopy Studies

The Nyquist plots were recorded for the SPE, MWCNT/SPE, MWCNT-CS/SPE, MWCNT-AgNP-CS/SPE, MWCNT-SG/SPE, MWCNT-AgNP-SG/SPE, MWCNT-1,8-DAN/SPE, and MWCNT-AgNP-1,8-DAN/SPE sensors using 0.1 M KCl solution containing 5 mM of $\text{Fe}(\text{CN})_6^{3-/4-}$ as redox probes (Figure 9). A sinusoidal potential modulation of 10 mV amplitude has been imposed at open circuit potential (OCP).

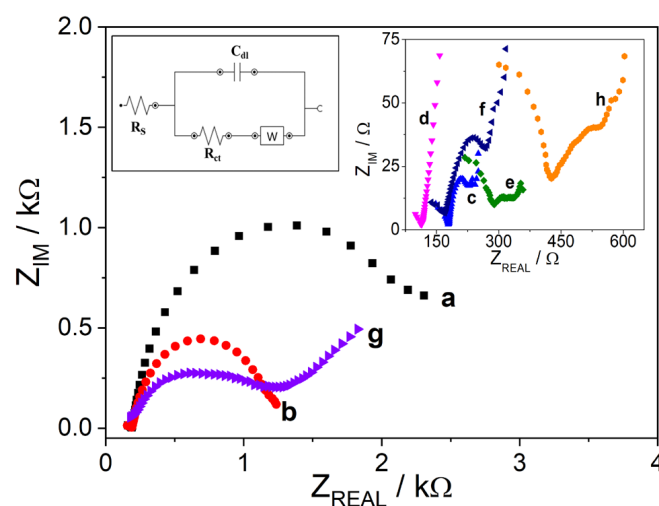


Figure 9. Nyquist plots registered for: (a) SPE, (b) MWCNT/SPE, (c) MWCNT-CS/SPE, (d) MWCNT-AgNP-CS/SPE, (e) MWCNT-SG/SPE, (f) MWCNT-AgNP-SG/SPE, (g) MWCNT-1,8-DAN/SPE, and (h) MWCNT-AgNP-1,8-DAN/SPE. Inset: Randles equivalent circuit (frequency range: 1 MHz–10 Hz, AC amplitude: 10 mV, OCP).

The impedance spectra were analyzed by fitting to equivalent electrical circuits using DropView 8400 software. The Randles equivalent circuit is presented in Figure 9 (inset) and contains the resistance of the electrolyte solution (R_s), the charge transfer resistance (R_{ct}), a capacitance (C_{dl}), and the Warburg diffusion element (W). The R_{ct} value indicates the resistance towards the electron transfer between the anions in the solution and the electrode surface.

The modification of the bare SPE with nanomaterials led to a decrease of the R_{ct} value from 2214 Ω for bare SPE, to 1215 Ω for MWCNT/SPE and 179 Ω for the MWCNT-CS/SPE sensors, which is correlated with an increase of the electron transfer between the sensor surface and the anionic species in the solution. The MWCNT layer ensures the conductivity of the electrode material, through a high surface area for interaction with the analyte, while the CS facilitates the absorption of the negatively charged anionic species. All these results demonstrate the synergistic effect of the MWCNT and CS towards the electrochemical detection of anionic species.

In the case of MWCNT-AgNP-CS/SPE, the R_{ct} value was calculated to be 162Ω , which indicates that the use of metallic nanoparticles did not yield a significant improvement of charge transfer properties.

For the sensors modified with nanomaterials based on polymeric film, a decrease of the R_{ct} values was observed when AgNPs were used, from a value of 968.78Ω for MWCNT-1,8-DAN/SPE to 340.96Ω for MWCNT-AgNP-1,8-DAN/SPE. This decrease can be explained by the electrocatalytic properties of the AgNPs, which increased the electron transfer at the surface of the sensor. Additionally, the lower R_{ct} value obtained for MWCNT-1,8-DAN/SPE compared with the one obtained for MWCNT/SPE is correlated with the presence of the positively charged amino groups on the 1,8-DAN monomer, which favor the electrostatic interaction with the $Fe(CN)_6^{3-/4-}$. However, the R_{ct} values for the sensors modified with polymer, with and without AgNP, were still higher than that of the MWCNT-CS/SPE sensor.

The lowest R_{ct} values, of 100Ω for MWCNT-SG/SPE and 147Ω for MWCNT-AgNP-SG/SPE, were obtained for SG-modified sensors, proving an enhancement of the electron transfer at the electrode surface, but correlated with the SEM studies, the SG matrix is not suitable to be used for further studies due to its poor stability, leading to a leaching of the nanomaterial layer in the solution.

Overall, the EIS studies showed that the MWCNT-CS/SPE have good charge transfer characteristics for the detection of anionic species in the solution due to the use of the MWCNTs together with CS.

3.4. Chronoamperometric Studies

Estimation of the catalytic rate constant (k_{cat}) and diffusion coefficient (D) for the electrocatalytic reaction was performed using chronoamperometry (Figure 10A–D). Chronoamperograms were recorded in acetate buffer containing 0.5, 1, and 2 mM of NO_2^- at 0.58 V on MWCNT-CS/SPE (Figure 10A). The ratio i_{cat}/i_{buffer} vs. the $t^{1/2}$ plot for 2 mM of nitrite represented in Figure 10B shows a linear variation used to calculate the catalytic rate constant.

The linear segments of plots i vs. $t^{-1/2}$ (Figure 10C) and slope vs. nitrite concentration (Figure 10D) were used for the calculation of the diffusion coefficient (D).

The catalytic constant, k_{cat} , was calculated with the equation:

$$\frac{i_{cat}}{i_{Buffer}} = \pi^{1/2} (k_{cat} C t)^{1/2} \quad (1)$$

where i_{cat} is the current recorded in the presence of analyte and i_{Buffer} represents the current recorded in the absence of the analyte, C is the concentration (mM) of nitrite, and t is the time (s).

The diffusion coefficient was calculated using the Cottrell Equation (2):

$$i = \frac{nFACD^{1/2}}{\pi^{1/2}t^{1/2}} \quad (2)$$

where I (μA) is the catalytic current of MWCNT-CS-based sensors in the presence of nitrite, F is the Faraday constant ($96,485 C/mol$), A is the area of the working electrode (cm^2), C is the concentration of NO_2^- , and n is the number of electrons transferred in the electrochemical reaction.

The catalytic constant value of $557.74 L \cdot mol^{-1} \cdot s^{-1}$, calculated by using the slope of the i_{cat}/i_{buffer} vs. $t^{1/2}$ plots recorded for 2 mM of nitrite (Figure 10B), was higher than that reported in the literature, of $45 L \cdot mol^{-1} \cdot s^{-1}$ for MnO_2 -decorated graphene oxide [40], demonstrating that MWCNT and CS act as an excellent catalyst toward the oxidation of nitrite. The obtained diffusion coefficient (D) was about $3.86 \times 10^{-6} cm^2 s^{-1}$.

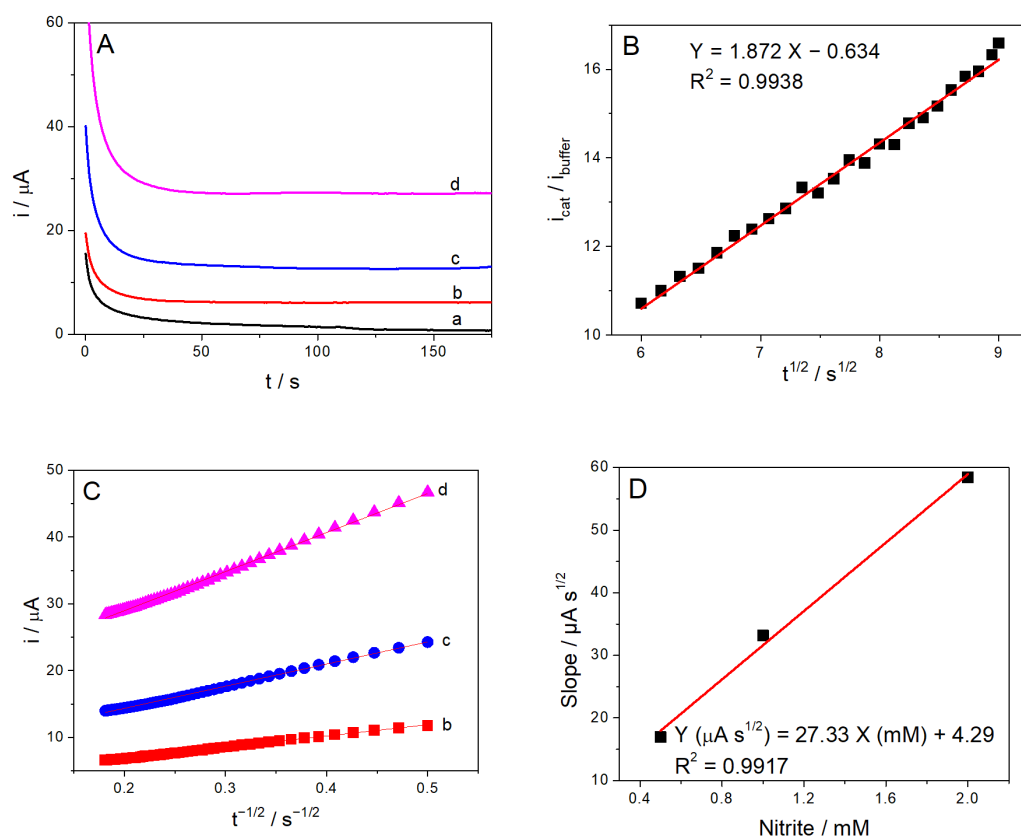


Figure 10. Chronoamperograms recorded for MWCNT-CS/SPE: (A) in the absence (a), and in the presence of 0.5 (b), 1 (c), and 2 mM (d) of nitrite. (B) i_{cat}/i_{Buffer} vs. the $t^{1/2}$ plot derived from (a) and (b). (C) Linear segments of plot i vs. $t^{-1/2}$ for 0.5, 1, and 2 mM of nitrite. (D) Plot of the slopes vs. the nitrite concentration.

3.5. Amperometric Detection of Nitrite Using MWCNT-CS/SPE Sensors

Taking into consideration the previous CV and EIS studies, the working conditions for the amperometric detection of nitrite were optimized by using MWCNT-CS/SPE sensors in a potential range of 0.53 to 0.65 V in acetate (pH 5) and PBS (pH 6–7) buffers of 0.1 M (Figure 11A). The analytical performances of the MWCNT-CS sensors at different pH values were obtained from the calibration curves using the linear regressions presented in Figure 11B.

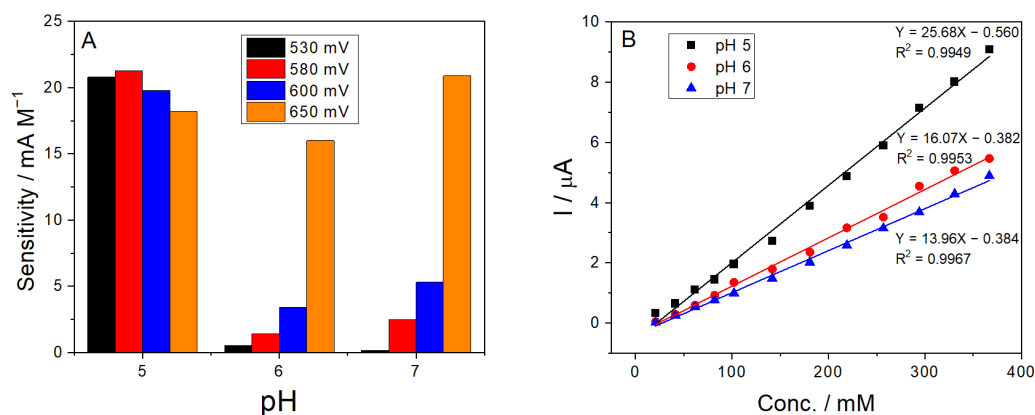


Figure 11. (A) Variation of the sensitivity with pH and applied working potentials for MWCNT-CS/SPE sensors. (B) Calibration curves for the amperometric detection of nitrite in acetate buffer, 0.1 M, pH 5, at an applied potential of 0.58 V, and in PBS, pH 6 and 7, at 0.68 V.

These results show that sensors based on MWCNT-CS presented better characteristics for the detection of nitrite in acidic medium (pH 5), at 0.58 V, with a specific sensitivity of $204.4 \text{ mA} \cdot \text{M}^{-1} \cdot \text{cm}^{-2}$ (RSD = 5.7%, $n = 5$) being obtained for a linear range of nitrite concentration up to 1.7 mM. The specific sensitivity obtained in neutral medium at 0.65 V was $111.1 \text{ mA} \cdot \text{M}^{-1} \cdot \text{cm}^{-2}$ (RSD = 8.6%, $n = 6$). Detection limits were determined for a S/N ratio of 3. The response time of MWCNT-CS-based sensors for the substrate was about 20 s in acidic medium, and respectively 32 s in neutral medium.

The analytical performance parameters of the MWCNT-CS/SPE sensor for nitrite detection were compared with other reported data from the literature, especially by using amperometric or DPV methods (Table 1).

Table 1. Comparison of the MWCNT-CS/SPE sensor with other amperometric sensors reported in the literature.

Sensor	pH	E_{ox} (V)	Linear Range (μM)	Sensitivity ($\text{mA M}^{-1} \text{cm}^{-2}$)	LOD (μM)	Sample	Ref.
Ag/Cu/MWNTs/GCE ^a	7.0	0.85	1–1000	-	0.2	lake and drinking water, seawater	[39]
AgNPs/MWCNTs/GCE	5.0	0.85	1–100	-	0.095	tap water	[38]
MnO ₂ /PANI ^b /GCE	5.0	0.85	19.98–732.17	225	1.08	tap and lake water	[34]
rGO-PANI-AsM ^c /GCE	4	0.83	25–7500	803	10.71	ground and sewage water	[37]
Pt-Cu/GO ^d /GCE	7.2	0.80	$0.2-9 \times 10^3$	139.9	3	-	[33]
ABC-800 ^e /GCE	-	0.73	4.9–1184	570	2.7	urine	[36]
NGE/PdNC ^f /GCE	6.0	0.73	$0.5-1.51 \times 10^3$	342.4	0.11	drinking water, sausage	[35]
AgMCs-PAA/PVA ^g /SPCE	7.0	0.70	2–800	474.14	4.5	meat products	[29]
Chit-TsCuPc ^h /GCE	4.0	0.55	0.05×10^{-2} -6.5×10^{-2}	4964×10^3	22×10^{-3}	chips, pickled vegetables	[24]
MnO ₂ /GO ⁱ -SPE	7.4	0.55	0.1–1, 1–1000	-	0.09	tap water, packaged water	[40]
MWCNT-CS/SPE	5.0 7.0	0.58 0.65	16–1700 20–1700	204.4 111.1	2.3 4.3	soil solutions	This work

^a Glassy carbon electrode, ^b polyaniline, ^c reduced graphene oxide-polyaniline-arsenomolybdate, ^d graphene oxide, ^e porous carbon synthesized at 800 °C, ^f nitrogen-doped graphene/palladium nano-cubes, ^g silver micro-cubics-polyacrylic acid/poly vinyl alcohol, ^h chitosan-protected tetra-sulfonated copper phthalocyanine, ⁱ manganese dioxide-decorated graphene oxide.

By using the MWCNT-CS-based sensors, it was possible to detect nitrite with good sensitivities and low detection limits in soil samples with different pH values, by working at relatively low values of applied potential, compared with the reported ones.

3.6. Stability, Reproducibility, and Interference Studies

The operational stability was estimated by measuring the sensor response to 0.1 mM of nitrite, rinsing the sensor after each measurement. The average current value was $1.38 \pm 0.07 \mu\text{A}$ by performing 10 successive substrate additions (RSD = 5.5%) in acetate buffer, 0.1 M, pH 5, at 0.58 V, and respectively, $1.25 \pm 0.08 \mu\text{A}$ (RDS = 5.8%) in PBS, 0.1 M, pH 7, at 0.65 V, suggesting a good operational stability of the developed sensors.

The long-term stability of the MWCNT-CS/SPE was estimated in the same conditions, by carrying out substrate determination during a seven-day period. The sensor showed a relatively stable response, with a variation of 4.2% for the amperometric response in acetate buffer, pH 5, and respectively, of 2.1% in PBS, pH 7.

Interference studies were carried out using possible interfering compounds, such as sodium nitrate, calcium chloride, magnesium chloride, urea, and glucose. Table 2 presents

the relative amperometric (%) response of the MWCNT-CS/SPE sensor recorded in 20 μM of sodium nitrite during successive additions of 20 μM of potential interfering species, expressed as the percentage of the initial response for nitrite, in acetate buffer at 0.58 V.

Table 2. Relative response (%) for 20 μM of nitrite in the presence of potential interfering compounds.

Compound	Relative Response (%)	RSD (%)
Na_2NO_3	89.5	3.9
CaCl_2	91.2	5.8
Urea	86.0	8.2
Glucose	93.0	7.5
Citric acid	89.5	7.8

It was observed that in the presence of the interfering species, the sensor response did not show a significant variation, with the highest value of the recorded current being obtained for sodium nitrite. The developed sensor proved high selectivity for the detection of nitrite in soil solution.

3.7. Detection of Nitrite in Real Samples

The MWCNT-CS/SPE sensors were used for the detection of nitrite content in different soil samples. Soils from corn fields and vegetable gardens were collected and used in the laboratory to grow tomatoes. Low-volume suction lysimeters were used to extract the soil solutions to be analyzed (Figure 12). The modified flexible sensors were easily integrated with a portable detector used in the field, which can gather and transmit data by wireless connection from multiple sampling points in an agriculture field, thus representing a promising tool for nitrite monitoring in food crops.

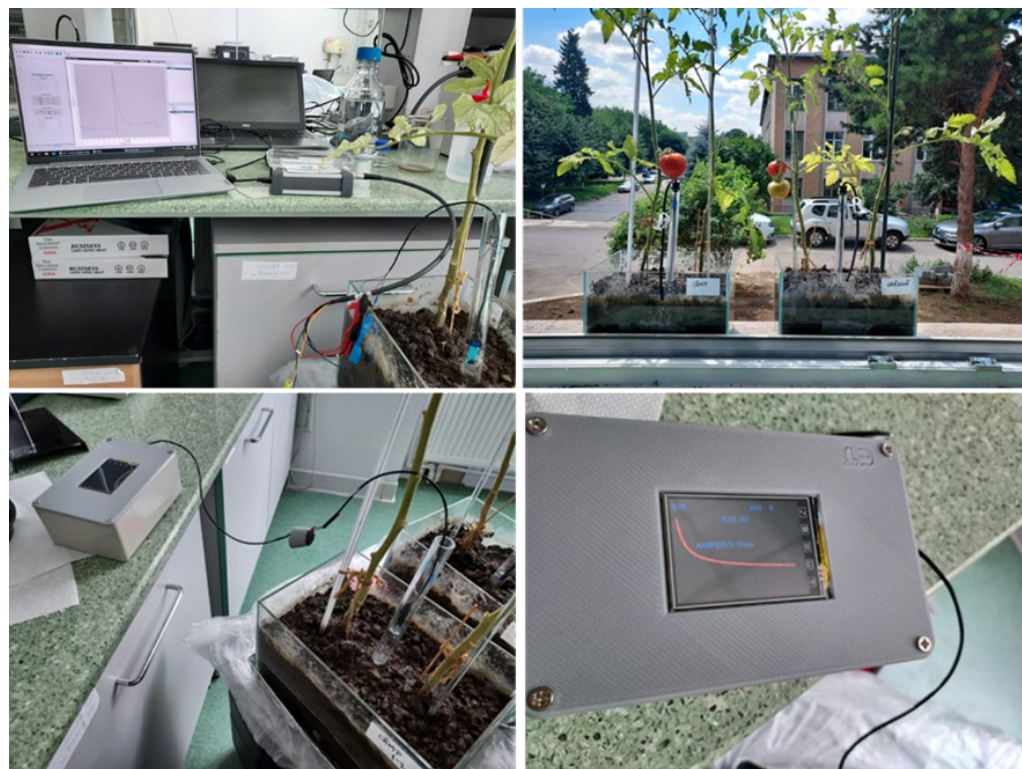


Figure 12. Nitrite determination in soil solutions using a portable miniaturized electrochemical detector and a flexible MWCNT-CS/SPE sensor.

Soil samples from agricultural lands and gardens were used for the determination of nitrite before culturing plants, and to monitor the variation of the nitrite concentration

before and after the cultivation of tomatoes. The soil containers were watered periodically and lysimeters were used to collect the soil solutions. Additionally, soil solutions were collected in-field.

Determination of nitrite contents by using the developed flexible sensors was performed by selecting the suitable calibration curve corresponding to the pH value of the soil samples. The results obtained with the developed sensors were compared with the results of colorimetric and spectrophotometric assays, showing a good correlation (Table 3).

Table 3. Determination of nitrite concentration (μM) from various soil solutions using different methods.

Soil	Determined Concentration of Nitrite (μM)		
	Spectrophotometric Measurement	Colorimetric Measurement	Amperometric Measurement
Field without plants, kept in the laboratory	56.5	52.9	45.6
Field with tomatoes, kept in the laboratory	10.7	8.6	7.4
Field with corn	68.7	55.3	55.2
Garden with tomatoes and eggplants	19.8	17.7	18
Garden without plants, kept in the laboratory	168.8	130.8	122
Garden with tomatoes, kept in the laboratory	20.4	22.9	18.9

The soil samples collected from the field and garden soils used for growing tomatoes in the laboratory were also used for measurements in spiked solutions (Table 4).

Table 4. Detection of nitrite in spiked soil samples.

Soil Samples	Nitrite Added (μM)	Nitrite Detected (μM)	Recovery (%)
Field	75	79	109.8 \pm 6.2
	125	138	110.3 \pm 8.2
Garden	75	81	107.7 \pm 6.5
	125	141	112.9 \pm 7.9

The recovery values between 107.7% and 112.9% demonstrate the reliability of the developed sensors.

The results obtained with the designed MWCNT-CS/SPE sensors were shown to be in good agreement with those achieved using reference methods.

4. Conclusions

A simple and low-cost method for the development of MWCNT-CS-based flexible sensors was used in order to ensure a sensitive, selective, and rapid determination of nitrite in soil solutions. The electrochemical properties of MWCNT-CS nanocomposite material towards nitrite oxidation were compared with different nanomaterials. Morpho-structural and electrochemical studies were used for the characterization and optimization of the nanomaterial-based sensor, in order to achieve a sensitive and selective determination of nitrite.

The developed flexible sensors were used for the determination of nitrite content in different soil samples, at low values of applied working potentials, which in this way reduced the influence of the potential interfering compounds.

Detection of nitrite in soil solutions was performed by using portable electrochemical detectors and flexible MWCNT-CS/SPE sensors, directly inserted in the suction lysimeters. It was proven that the combination of MWCNT and CS ensured high sensitivity, accuracy, selectivity, and stability for nitrite detection in real samples.

This flexible and portable system developed for nitrite detection was successfully tested for transmission of recorded data in-field to our laboratory access point, by using a wireless communication system developed by our partner EPI-SISTEM.

This simple and cost-effective preparation method of the nanocomposite-based sensors can be easily adapted for different types of potential contaminants in soil.

Supplementary Materials: The following supporting information can be downloaded at: <https://www.mdpi.com/article/10.3390/chemosensors11040224/s1>, Figure S1: SEM images of: (A) MWCNT-AgNP/SPE; (B) MWCNT-AgNP-CS/SPE; (C) MWCNT-SG/SPE; (D) MWCNT-AgNP-SG/SPE; (E) 1,8-DAN/SPE; (F) MWCNT-1,8-DAN/SPE and (G) MWCNT-AgNP-1,8-DAN/SPE. Figure S2: Cyclic voltammograms recorded for: MWCNT-AgNP/SPE (a), MWCNT-AgNP-CS/SPE (b), MWCNT-AgNP-1,8-DAN/SPE (c) and MWCNT-AgNP-SG/SPE (d). (PBS 0.1M, pH 7, $v = 0.05$ V/s).

Author Contributions: Conceptualization, A.-M.G., L.-G.Z., and M.D.; methodology, A.-M.G., M.-L.J., and M.D.; software, L.-G.Z. and P.E.; validation, A.-M.G., L.-G.Z., M.L.J., I.-R.Ș.-B., and R.M.S.; formal analysis, L.-G.Z., I.-R.Ș.-B., R.M.S., and M.L.J.; investigation, I.-R.Ș.-B., R.M.S., and M.-L.J.; resources, P.E. and M.L.J.; data curation, A.-M.G., L.-G.Z., P.E., and M.L.J.; writing—original draft preparation, A.-M.G. and L.-G.Z.; writing—review and editing, A.-M.G. and M.D.; visualization, A.-M.G., P.E., and M.D.; supervision, A.-M.G. and M.D.; project administration, M.D. All authors have read and agreed to the published version of the manuscript.

Funding: This research was funded by the Romanian National Authority for Scientific Research and Innovation, CCCDI—UEFISCDI, through ERANET-MANUNET-NITRISENS no. 216/2020, within PNCDI III.

Institutional Review Board Statement: Not applicable.

Informed Consent Statement: Not applicable.

Data Availability Statement: Not applicable.

Acknowledgments: The support provided by the Ministry of Research, Innovation, and Digitization through Core Program PN19.23.03.02 and Program 1—Development of the national research and development system, Subprogram 1.2—Institutional performance—Projects to finance excellence in RDI, Contract No. 15PFE/2021, is also gratefully acknowledged. L.-G.Z.'s fellowship was also supported by the Romanian Young Academy, funded by Stiftung Mercator and the Alexander von Humboldt Foundation for the period 2020–2022. The authors gratefully acknowledge the support of Iuliana Raut and Mariana Constantin (National Institute for Research and Development in Chemistry and Petrochemistry—ICECHIM Bucharest) for the microbial studies regarding the soil microbiota involved in nitrite production.

Conflicts of Interest: The authors declare no conflict of interest.

References

1. Beeckman, F.; Motte, H.; Beeckman, T. Nitrification in agricultural soils: Impact, actors and mitigation. *Curr. Opin. Biotechnol.* **2018**, *50*, 166–173. [[CrossRef](#)] [[PubMed](#)]
2. Liu, Z.; Manikandan, V.S.; Chen, A. Recent advances in nanomaterial-based electrochemical sensing of nitric oxide and nitrite for biomedical and food research. *Curr. Opin. Electrochem.* **2019**, *16*, 127–133. [[CrossRef](#)]
3. El hani, O.; Karrat, A.; Digua, K.; Amine, A. Development of a simplified spectrophotometric method for nitrite determination in water samples. *Spectrochim. Acta A Mol. Biomol. Spectrosc.* **2022**, *267*, 120574. [[CrossRef](#)] [[PubMed](#)]
4. Zhang, K.; Li, S.; Liu, C.; Wang, Q.; Wang, Y.; Fan, J. A hydrophobic deep eutectic solvent-based vortex-assisted dispersive liquid–liquid microextraction combined with HPLC for the determination of nitrite in water and biological samples. *J. Sep. Sci.* **2019**, *42*, 574–581. [[CrossRef](#)]
5. Murray, E.; Roche, P.; Briet, M.; Moore, B.; Morrin, A.; Diamond, D.; Paull, B. Fully automated, low-cost ion chromatography system for in-situ analysis of nitrite and nitrate in natural waters. *Talanta* **2020**, *216*, 120955. [[CrossRef](#)]
6. Ma, Z.; Li, J.; Hu, X.; Cai, Z.; Dou, X. Ultrasensitive, Specific, and Rapid Fluorescence Turn-On Nitrite Sensor Enabled by Precisely Modulated Fluorophore Binding. *Adv. Sci.* **2020**, *7*, 2002991. [[CrossRef](#)]
7. Han, S.; Chen, X. Copper nanoclusters-enhanced chemiluminescence for folic acid and nitrite detection. *Spectrochim. Acta A Mol. Biomol. Spectrosc.* **2019**, *210*, 315–320. [[CrossRef](#)] [[PubMed](#)]
8. Moravský, L.; Troška, P.; Klas, M.; Masár, M.; Matejčík, Š. Determination of nitrites and nitrates in plasma-activated deionized water by microchip capillary electrophoresis. *Contrib. Plasma Phys.* **2020**, *60*, e202000014. [[CrossRef](#)]

9. Ryu, H.; Thompson, D.; Huang, Y.; Li, B.; Lei, Y. Electrochemical sensors for nitrogen species: A review. *Sens. Actuators Rep.* **2020**, *2*, 100022. [[CrossRef](#)]
10. Galloway, J.N.; Townsend, A.R.; Erisman, J.W.; Bekunda, M.; Cai, Z.; Freney, J.R.; Martinelli, L.A.; Seitzinger, S.P.; Sutton, M.A. Transformation of the Nitrogen Cycle: Recent Trends, Questions, and Potential Solutions. *Science* **2008**, *320*, 889–892. [[CrossRef](#)]
11. Lin, P.; Chai, F.; Zhang, R.; Xu, G.; Fan, X.; Luo, X. Electrochemical synthesis of poly(3,4-ethylenedioxythiophene) doped with gold nanoparticles, and its application to nitrite sensing. *Microchim. Acta* **2016**, *183*, 1235–1241. [[CrossRef](#)]
12. Fan, X.; Lin, P.; Liang, S.; Hui, N.; Zhang, R.; Feng, J.; Xu, G. Gold nanoclusters doped poly(3,4-ethylenedioxythiophene) for highly sensitive electrochemical sensing of nitrite. *Ionics* **2017**, *23*, 997–1003. [[CrossRef](#)]
13. Quan, D.; Shin, W. A Nitrite Biosensor Based on Co-immobilization of Nitrite Reductase and Viologen-modified Chitosan on a Glassy Carbon Electrode. *Sensors* **2010**, *10*, 6241–6256. [[CrossRef](#)] [[PubMed](#)]
14. Monteiro, T.; Rodrigues, P.R.; Gonçalves, A.L.; Moura, J.J.G.; Jubete, E.; Añorga, L.; Píknova, B.; Schechter, A.N.; Silveira, C.M.; Almeida, M.G. Construction of effective disposable biosensors for point of care testing of nitrite. *Talanta* **2015**, *142*, 246–251. [[CrossRef](#)]
15. Badea, M.; Amine, A.; Paleschi, G.; Moscone, D.; Volpe, G.; Curulli, A. New electrochemical sensors for detection of nitrites and nitrates. *J. Electroanal. Chem.* **2001**, *509*, 66–72. [[CrossRef](#)]
16. Badea, M.; Amine, A.; Benzine, M.; Curulli, A.; Moscone, D.; Lupu, A.; Volpe, G.; Paleschi, G. Rapid and Selective Electrochemical Determination of Nitrite in Cured Meat in the Presence of Ascorbic Acid. *Microchim. Acta* **2004**, *147*, 51–58. [[CrossRef](#)]
17. Yang, Z.; Zhou, X.; Yin, Y.; Fang, W. Determination of Nitrite by Noble Metal Nanomaterial-Based Electrochemical Sensors: A Minireview. *Anal. Lett.* **2021**, *54*, 2826–2850. [[CrossRef](#)]
18. Baig, N.; Sajid, M.; Saleh, T.A. Recent trends in nanomaterial-modified electrodes for electroanalytical applications. *TrAC Trends Anal. Chem.* **2019**, *111*, 47–61. [[CrossRef](#)]
19. Oliveira, T.M.B.F.; Morais, S. New Generation of Electrochemical Sensors Based on Multi-Walled Carbon Nanotubes. *Appl. Sci.* **2018**, *8*, 1925. [[CrossRef](#)]
20. Munawar, A.; Ong, Y.; Schirhagl, R.; Tahir, M.A.; Khan, W.S.; Bajwa, S.Z. Nanosensors for diagnosis with optical, electric and mechanical transducers. *RSC Adv.* **2019**, *9*, 6793–6803. [[CrossRef](#)]
21. Li, Y.; Chen, Y.; Yu, H.; Tian, L.; Wang, Z. Portable and smart devices for monitoring heavy metal ions integrated with nanomaterials. *TrAC Trends Anal. Chem.* **2018**, *98*, 190–200. [[CrossRef](#)]
22. Li, X.; Ping, J.; Ying, Y. Recent developments in carbon nanomaterial-enabled electrochemical sensors for nitrite detection. *TrAC Trends Anal. Chem.* **2019**, *113*, 1–12. [[CrossRef](#)]
23. Prabhu, A.; Crapnell, R.D.; Eersels, K.; van Grinsven, B.; Kunhiraman, A.K.; Singla, P.; McClements, J.; Banks, C.E.; Novakovic, K.; Peeters, M. Reviewing the use of chitosan and polydopamine for electrochemical sensing. *Curr. Opin. Electrochem.* **2022**, *32*, 100885. [[CrossRef](#)]
24. Sudarvizhi, A.; Pandian, K.; Oluwafemi, O.S.; Gopinath, S.C.B. Amperometry detection of nitrite in food samples using tetrasulfonated copper phthalocyanine modified glassy carbon electrode. *Sens. Actuators B Chem.* **2018**, *272*, 151–159. [[CrossRef](#)]
25. Rao, H.; Liu, Y.; Zhong, J.; Zhang, Z.; Zhao, X.; Liu, X.; Jiang, Y.; Zou, P.; Wang, X.; Wang, Y. Gold Nanoparticle/Chitosan@N,S Co-doped Multiwalled Carbon Nanotubes Sensor: Fabrication, Characterization, and Electrochemical Detection of Catechol and Nitrite. *ACS Sustain. Chem. Eng.* **2017**, *5*, 10926–10939. [[CrossRef](#)]
26. Bibi, S.; Zaman, M.I.; Niaz, A.; Rahim, A.; Nawaz, M.; Bilal Arian, M. Voltammetric determination of nitrite by using a multiwalled carbon nanotube paste electrode modified with chitosan-functionalized silver nanoparticles. *Microchim. Acta* **2019**, *186*, 595. [[CrossRef](#)]
27. Sakhuja, N.; Jha, R.; Laha, S.S.; Rao, A.; Bhat, N. Fe₃O₄ Nanoparticle-Decorated WSe₂ Nanosheets for Selective Chemiresistive Detection of Gaseous Ammonia at Room Temperature. *ACS Appl. Nano Mater.* **2020**, *3*, 11160–11171. [[CrossRef](#)]
28. Bao, Z.; Zhong, H.; Li, X.; Zhang, A.; Liu, Y.; Chen, P.; Cheng, Z.; Qian, H.-y. Core-shell Au@Ag nanoparticles on carboxylated graphene for simultaneous electrochemical sensing of iodide and nitrite. *Sens. Actuators B Chem.* **2021**, *345*, 130319. [[CrossRef](#)]
29. Promsuwan, K.; Thavarungkul, P.; Kanatharana, P.; Limbut, W. Flow injection amperometric nitrite sensor based on silver microcubics-poly (acrylic acid)/poly (vinyl alcohol) modified screen printed carbon electrode. *Electrochim. Acta* **2017**, *232*, 357–369. [[CrossRef](#)]
30. Duan, C.; Bai, W.; Zheng, J. Non-enzymatic sensors based on a glassy carbon electrode modified with Au nanoparticles/polyaniline/SnO₂ fibrous nanocomposites for nitrite sensing. *New J. Chem.* **2018**, *42*, 11516–11524. [[CrossRef](#)]
31. Arulraj, A.D.; Sundaram, E.; Vasantha, V.S.; Neppolian, B. Polypyrrole with a functionalized multi-walled carbon nanotube hybrid nanocomposite: A new and efficient nitrite sensor. *New J. Chem.* **2018**, *42*, 3748–3757. [[CrossRef](#)]
32. Xu, H. Ultrasensitive Detection of Nitrite Based on gold-nanoparticles/ Polyrhodamine B/Carbon Nanotubes Modified Glassy Carbon Electrode with Enhanced Electrochemical Performance. *Int. J. Electrochem. Sci.* **2017**, *12*, 10642–10659. [[CrossRef](#)]
33. Li, Y.; Zhang, X.; Zheng, J. One-pot aqueous method for facile synthesis of platinum-copper bimetallic catalyst based on graphene oxide and its highly enhanced sensing of nitrite. *J. Mater. Sci. Mater. Electron.* **2020**, *31*, 13301–13309. [[CrossRef](#)]
34. Qiu, Y.; Qu, K. Binary organic-inorganic nanocomposite of polyaniline-MnO₂ for non-enzymatic electrochemical detection of environmental pollutant nitrite. *Environ. Res.* **2022**, *214*, 114066. [[CrossRef](#)] [[PubMed](#)]

35. Shen, Y.; Rao, D.; Bai, W.; Sheng, Q.; Zheng, J. Preparation of high-quality palladium nanocubes heavily deposited on nitrogen-doped graphene nanocomposites and their application for enhanced electrochemical sensing. *Talanta* **2017**, *165*, 304–312. [[CrossRef](#)]
36. Sudha, V.; Senthil Kumar, S.M.; Thangamuthu, R. Hierarchical porous carbon derived from waste amla for the simultaneous electrochemical sensing of multiple biomolecules. *Colloids Surf. B* **2019**, *177*, 529–540. [[CrossRef](#)]
37. Suma, B.P.; Adarakatti, P.S.; Kempahanumakkagari, S.K.; Malingappa, P. A new polyoxometalate/rGO/Pani composite modified electrode for electrochemical sensing of nitrite and its application to food and environmental samples. *Mater. Chem. Phys.* **2019**, *229*, 269–278. [[CrossRef](#)]
38. Wan, Y.; Zheng, Y.F.; Wan, H.T.; Yin, H.Y.; Song, X.C. A novel electrochemical sensor based on Ag nanoparticles decorated multi-walled carbon nanotubes for applied determination of nitrite. *Food Control* **2017**, *73*, 1507–1513. [[CrossRef](#)]
39. Zhang, Y.; Nie, J.; Wei, H.; Xu, H.; Wang, Q.; Cong, Y.; Tao, J.; Zhang, Y.; Chu, L.; Zhou, Y.; et al. Electrochemical detection of nitrite ions using Ag/Cu/MWNT nanoclusters electrodeposited on a glassy carbon electrode. *Sens. Actuators B Chem.* **2018**, *258*, 1107–1116. [[CrossRef](#)]
40. Jaiswal, N.; Tiwari, I.; Foster, C.W.; Banks, C.E. Highly sensitive amperometric sensing of nitrite utilizing bulk-modified MnO₂ decorated Graphene oxide nanocomposite screen-printed electrodes. *Electrochim. Acta* **2017**, *227*, 255–266. [[CrossRef](#)]
41. EPA Method 354.1. Available online: <https://settek.com/EPA-Method-354-1/> (accessed on 23 February 2023).
42. Ayad, M.M.; Salahuddin, N.A.; Minisy, I.M.; Amer, W.A. Chitosan/polyaniline nanofibers coating on the quartz crystal microbalance electrode for gas sensing. *Sens. Actuators B Chem.* **2014**, *202*, 144–153. [[CrossRef](#)]
43. Qi, P.; Xu, Z.; Zhang, T.; Fei, T.; Wang, R. Chitosan wrapped multiwalled carbon nanotubes as quartz crystal microbalance sensing material for humidity detection. *J. Colloid Interface Sci.* **2020**, *560*, 284–292. [[CrossRef](#)] [[PubMed](#)]
44. Nasalska, A.; Skompska, M. Removal of toxic chromate ions by the films of poly(1,8-diaminonaphthalene). *J. Appl. Electrochem.* **2003**, *33*, 113–119. [[CrossRef](#)]
45. Keita, B.; Belhouari, A.; Nadjo, L.; Contant, R. Electrocatalysis by polyoxometalate/vb polymer systems: Reduction of nitrite and nitric oxide. *J. Electroanal. Chem.* **1995**, *381*, 243–250. [[CrossRef](#)]
46. Afkhami, A.; Soltani-Felehgari, F.; Madrakian, T.; Ghaedi, H. Surface decoration of multi-walled carbon nanotubes modified carbon paste electrode with gold nanoparticles for electro-oxidation and sensitive determination of nitrite. *Biosens. Bioelectron.* **2014**, *51*, 379–385. [[CrossRef](#)]
47. Piela, B.; Wrona, P.K. Oxidation of Nitrites on Solid Electrodes: I. Determination of the Reaction Mechanism on the Pure Electrode Surface. *J. Electrochem. Soc.* **2002**, *149*, E55. [[CrossRef](#)]

Disclaimer/Publisher’s Note: The statements, opinions and data contained in all publications are solely those of the individual author(s) and contributor(s) and not of MDPI and/or the editor(s). MDPI and/or the editor(s) disclaim responsibility for any injury to people or property resulting from any ideas, methods, instructions or products referred to in the content.